

# **Evaluation of Selected Empirical Schemes of Calculating Sensible Heat Flux from Routinely-Measured Meteorological Parameters in a Tropical Location**

## **ABSTRACT**

The accurate estimation of sensible heat flux ( $H_s$ ) is imperative in the exchange of energy and mass between the earth's systems. However, the process of acquiring the sensible heat flux data is challenging due to the complexity in its direct measurement hence, not readily available. The alternative is to use estimations which are derived from specific models. This study evaluated the performances of five selected schemes of estimating  $H_s$  from routinely-measured meteorological parameters using statistical methods such as Mean Bias Error (MBE), Mean Percentage Difference (MPD), Root Mean Square Error (RMSE), Index of Agreement (IA), Correlation Coefficient (R) and Coefficient of Determination ( $R^2$ ). The empirical schemes selected are: Berkowicz and Prahm (BP), Bowen Ratio Energy Balance (BREB), Holstlag and Van Ulden (HU), Smith (ST) and Surface Temperature (ST) schemes. The results obtained revealed that in the dry season, MBE values of  $6.9 \text{ Wm}^{-2}$ ,  $7.2 \text{ Wm}^{-2}$ ,  $7.5 \text{ Wm}^{-2}$ ,  $6.3 \text{ Wm}^{-2}$  and  $-3.8 \text{ Wm}^{-2}$  were obtained for BP, BREB, HU, SMT and ST respectively. In the wet season, BP, BREB, HU, SMT and ST had MBE values of  $37.4 \text{ Wm}^{-2}$ ,  $14.2 \text{ Wm}^{-2}$ ,  $4.2 \text{ Wm}^{-2}$ ,  $12.0 \text{ Wm}^{-2}$  and  $-1.1 \text{ Wm}^{-2}$  respectively. The MBEs, RMSEs and MPDs obtained for the schemes were higher in the wet season (about 70 %) than in the dry season; implying that the schemes performed better in the dry season than in the wet season. The study rated BREB as the best method of estimating the sensible heat flux at the study location having the lowest MBE, lowest MPD, lowest RMSE, high R, high  $R^2$  and high IA in both seasons.

*Keywords: Sensible Heat Flux, Meteorological Parameters, Dry season, Wet season*

## 1. INTRODUCTION

The turbulent heat fluxes (sensible and latent heat fluxes) are the main components in the exchange of energy between the land surface and atmosphere [1,2]. They regulate the development and features of the planetary boundary layer, such as: the surface temperature, humidity and thermodynamic behaviour [3,4]. The sensible heat flux ( $H_s$ ) at the earth's surface is the energy transfer between the surface and the overlying atmosphere and mainly depends on the temperature difference between the surface and the air. It is largely responsible for the convective dry heat transfer within the atmospheric boundary layer. The sensible heat flux can either increase or decrease energy at the surface subject to the prevailing meteorological conditions and the surface temperature.  $H_s$  is normally directed away from the surface at day time as a result of the surface being warmer than the air above it and vice versa at night time [5]. It is the sensible heat flux at the surface that provides the heat energy that drives most atmospheric air motion that can be quantified for the estimation of air pollution dispersion (from anthropogenic sources such as transportation, industrial activities, etc.), thermal conditions for soil-plant-atmosphere system, crop weather modelling, etc [6]. A research by Katavoutas *et al.* [7], reported a dependence of human comfort on the surface convective heat fluxes, therefore, the role of the sensible heat flux in the tropospheric processes cannot be overemphasized. The sensible heat flux,  $H_s$  can be expressed as:

$$H_s = \rho c_p k_h \frac{\partial T}{\partial z} \quad (1)$$

where  $\rho$  is air density,  $c_p$  is the specific heat capacity at constant pressure,  $K_h$  is Eddy diffusivity of heat,  $\partial T$  is the change in temperature and  $\partial z$  is the change in height.

Obtaining accurate estimates of sensible heat flux is essential for understanding the atmospheric boundary layer stability and numerical weather forecasting. The most commonly used instruments for the direct measurement of sensible heat flux are the Eddy Covariance (EC) System and Large Aperture Scintillometer (LAS). The EC method

is assumed to be the most accurate method for the determination of turbulent heat fluxes [8]. Fluxes are measured as the covariance between fluctuations of vertical wind speed ( $w'$ ) and sonic virtual temperature ( $T'_s$ ) yielding the sensible heat flux, i.e.

$$H_s = -\rho c_p \overline{w' T'_s} \quad (2)$$

where  $\rho$  is air density,  $c_p$  is the specific heat capacity at constant pressure. However, the instrument has a lot of limitations such as co-ordinate rotation, sensitivity to fetch, finite flux averaging, trained personnel, etc [9,10,11]. LAS uses the propagation theory of an electromagnetic radiation pulse to measure the strength of the refractive index of air and the structure parameter of the refractive index ( $C_n^2$ ) and then relates it to the structure function parameter of temperature ( $C_T^2$ ) to derive the sensible heat flux, i.e.

$$C_T^2 = C_n^2 \left( \frac{T^2}{-0.78 \times 10^{-6} P} \right)^2 \left( 1 + \frac{0.03}{\beta} \right)^{-2} \quad (3)$$

where  $T$  is the air temperature,  $P$  is the atmospheric pressure and  $\beta$  is the Bowen ratio. The major limitation of this technique is that it depends on the semi empirical Monin-Obukhov similarity theory (MOST) for the determination of fluxes [12]. Due to the complexities in the direct measurements of sensible heat flux, the substitute is to derive the heat flux from empirical formulae. The input data used for the empirical formulae are sourced from routinely-measured meteorological parameters. The routinely-measured meteorological parameters such as solar radiation, air temperature, relative humidity, wind speed are commonly (easily) measured at meteorological stations. However, there have been discrepancies when applying the formulae to other data derived from geographical locations with atmospheric conditions that are different from the original locations. Improvement and analysis of methods for estimating heat fluxes that are reliable and simple to apply are important in micrometeorological research. Therefore, the purpose of this study is to evaluate and validate the existing schemes with the aim of improving their performances in a tropical location.

## 2. THEORY AND METHODOLOGY

### 2.1 Estimations of Sensible Heat Flux from Routinely-Measured Meteorological Parameters

Many indirect techniques have been formulated to calculate the sensible heat flux,  $H_s$ , using observations of meteorological variables measured in-situ or remotely. The schemes are based on experimental data with comprehensive study of the weather and the physical processes involved. The meteorological data used in this study such as solar radiation, air temperature, soil temperature, wind speed and relative humidity were sourced from the routine measurements made at the meteorological station. Other parameters such as friction velocity, ground heat flux, humidity deficit, roughness lengths used in the calculation of  $H_s$  were derived from the above-mentioned routinely-measured meteorological variables. The period of estimation was between 2016 and 2018.

The following methods of estimation of  $H_s$  were evaluated in this study: The aerodynamic resistance schemes such as: Berkowicz and Prahm (BP) scheme, Holtslag and Van Ulden (HU) scheme, Smith (SMT) scheme and Surface Temperature (ST) scheme; and the Bowen Ratio Energy Balance (BREB) method. The choice of selecting these schemes was due to the availability of data for the various input parameters. The results obtained from the schemes were compared with the experimental data.

#### 2.2.1 Berkowicz and Prahm Heat Flux Scheme

The Berkowicz and Prahm (BP) scheme [13] of estimating  $H_s$  can be expressed as:

$$H_s = \frac{R_a(r_a + r_s) - \delta q \rho c_p / \gamma}{\frac{4}{3r_s} + (\frac{4}{3} + \Delta/\gamma)r_a} \quad (4)$$

where  $R_a = R_n - H_g$ ;  $R_n$  is the net radiation;  $H_g$  is the soil heat flux;  $\rho$  is the density of air;  $c_p$  is the specific heat capacity of air;  $\delta q$  is the humidity deficit;  $r_a$  and  $r_s$  are the aerodynamic and surface resistances;  $\gamma$  is the psychrometric constant;  $\Delta = de_s/dT$  and  $e_s$  is the saturated vapour pressure. The BP approach is centred on the Monin-Obukhov similarity theory using the following equations:

$$r_a = \frac{0.74}{ku_*} \left[ \ln\left(\frac{Z_T}{Z_0}\right) - \psi_h\left(\frac{Z_T}{L}\right) + \psi_h\left(\frac{Z_0}{L}\right) \right] \quad (5)$$

$$r_s = \delta q \rho c_p / \gamma \delta \quad (6)$$

where  $Z_T$  is the measurement height of temperature;  $Z_0$  is the roughness length;  $k$  is von Karman's constant;  $u_*$  is the friction velocity.

$$\delta = 0.25R_n + A \quad (7)$$

where  $R_n$  is the net radiation and  $A$  is an arbitrary number that depends on vegetation type.

### 2.2.2 Bowen Ratio Energy Balance (BREB)

The Bowen Ratio Energy Balance (BREB) method is an indirect method of estimating sensible and latent heat fluxes at the surface [14,15]. High positive values of Bowen ratio indicate high sensible heating and low evapotranspiration [16]. On the contrary, low values of Bowen ratio (almost zero), indicate that most of the available energy is used for evapotranspiration (latent heat).

The BREB method breaks down when the estimated Bowen ratio value is within the range:  $-1.25 < \beta < -0.75$ . This is typical of dusk and dawn conditions at the surface [17]. In order to appropriately resolve the ratio, Foken *et al.* [18], suggested that the temperature gradient should be greater than the range of values between 4 and 8. Practically, such criteria are rarely considered since the aerodynamical heights of high vegetation are about 1.5 [19,20]. The main disadvantage of using the BREB technique is in the non-closure equation of the surface energy balance. The residual energy is usually summed up with the net radiation or distributed to the sensible and latent heat fluxes. Therefore, the energy fluxes estimated using BREB are usually higher than those determined with the EC method [18]. The surface energy balance can be stated as:

$$R_n = H_s + H_L + H_G \quad (8)$$

where  $R_n$  is the net radiation;  $H_S$  is the sensible heat flux;  $H_L$  is the latent heat flux and  $H_G$  is the downward ground heat flux. The net radiation  $R_n$  can be expressed as:

$$R_n = (1 - \alpha)R_{s\downarrow} + R_{l\downarrow} - R_{l\uparrow} \quad (9)$$

where  $\alpha$  is the surface albedo,  $R_{s\downarrow}$  is the incoming solar radiation,  $R_{l\downarrow}$  is the incoming longwave radiation and  $R_{l\uparrow}$  is the outgoing longwave radiation.

$$R_{s\downarrow} = I_{toa}(\lambda)e^{AM_\theta} \quad (10)$$

$$R_{l\downarrow} = \varepsilon_a \sigma T_a^4 \quad (11)$$

$$R_{l\uparrow} = \varepsilon_o \sigma T_s^4 \quad (12)$$

where  $I_{toa}$  is the radiation at the top of the atmosphere,  $AM_\theta$  is the air mass at solar zenith angle  $\theta$ ;  $\varepsilon_a$  and  $\varepsilon_o$  are the atmospheric and surface emissivity respectively;  $T_a$  and  $T_s$  are the air and surface temperatures respectively and  $\sigma$  is Stefan-Boltzmann's constant.

The available energy ( $R_n - H_G$ ) which is the deficit of the ground heat flux from the net radiation, is partitioned into sensible heat flux and latent heat flux as:

$$H_S = \frac{R_n - H_G}{1 + \beta^{-1}} \quad (13)$$

$$H_L = \frac{R_n - H_G}{1 + \beta} \quad (14)$$

$$H_G = -C \frac{\Delta T}{\Delta Z} \quad (15)$$

where  $C$  is the thermal conductivity of the soil,  $\Delta T$  is the change in soil temperature at soil depths  $Z_1$  and  $Z_2$ . Therefore, the Bowen ratio can be written as:

$$\beta = \frac{H_S}{H_L} = \gamma \frac{\Delta T}{\Delta e} \quad (16)$$

where  $\gamma$  is the Psychrometric constant =  $0.0667 \text{ hPaK}^{-1}$ ,  $\Delta T$  is the change in air temperature between heights  $Z_1$  and  $Z_2$  and  $\Delta e$  is the vapour pressure change at the same temperature.

### 2.2.3 Holtslag and Van Ulden (HU) Heat Flux Scheme

The Holtslag and Van Ulden (HU) heat flux scheme [21] can be used to estimate the sensible heat flux as:

$$H_s = \frac{(1-\alpha)+(\gamma/s)}{1+(\gamma/s)} (R_n - H_G) - \sigma \quad (17)$$

where  $R_n$  is the net radiation,  $H_G$  is the ground heat flux,  $s = dq_s/dT$ ,  $q_s$  being the saturated specific humidity;  $\gamma = c_p/\lambda$ ,  $\lambda$  = the specific latent heat of vaporization of water. The empirical parameters  $\alpha$  and  $\sigma$  vary with different soil moisture conditions.

### 2.2.4 Smith Heat Flux Scheme

The Smith heat flux scheme can be used to calculate sensible heat flux as proposed by Smith [22]:

$$H_s = \frac{R_a(r_a + r_s) - \delta q \rho c_p / \gamma}{(1 + \Delta/\gamma)r_a + r_s} \quad (18)$$

where  $R_a = R_n - H_G$  (19)

where  $R_n$  is the net radiation,  $H_G$  is the ground heat flux,  $\rho$  is the density of air,  $c_p$  is the specific heat capacity of air,  $\delta q$  is the humidity deficit  $= \left(1 - \frac{h}{100}\right) e_s(T)$ ,  $h$  is the relative humidity (%) and  $e_s(T)$  is the saturated vapour pressure as a function of temperature ( $T$ ),  $r_a$  and  $r_s$  are the aerodynamic and surface resistances,  $\gamma$  is the psychrometric constant and  $\Delta = de_s/dT$ .

### 2.2.5 Surface Temperature (ST) Scheme

The surface temperature method can be used to determine the sensible heat flux when the difference between the aerodynamic surface and radiometric temperatures is considered [23]. It can be achieved by the addition of an excess resistance to the

aerodynamic resistance. The expression for the sensible heat flux using the surface temperature scheme is as follows:

$$H_s = \frac{\rho c_p (T_s - T_a)}{r_h} \quad (20)$$

where  $\rho$  is the density of dry air;  $c_p$  is the specific heat of dry air;  $T_a$  is the air temperature at reference height  $Z$  and  $r_h$  is the resistance of heat transfer from a surface at temperature  $T_s$ . The resistance ( $r_h$ ) is the sum of the aerodynamic resistance ( $r_a$ ) of heat transfer from the surface to height  $z$  and an excess resistance ( $r_r$ )

$$r_h = r_a + r_r \quad (21)$$

where

$$r_a = \frac{1}{k^2 u} \left[ \ln \left( \frac{z-d}{z_{0m}} \right) \ln \left( \frac{z-d}{z_{0h}} \right) \right] \quad (22)$$

and

$$r_r = \frac{B^{-1}}{u_*} = \ln \left( \frac{z_{0m}}{z_{0h}} \right) / k u_* \quad (23)$$

where  $k$  is the von Karman's constant = 0.4,  $u_*$  is the friction velocity,  $d$  is the zero-plane displacement,  $z_{0m}$  and  $z_{0h}$  are the roughness lengths for momentum and heat respectively.

The excess resistance  $r_r$  is often expressed in terms of  $kB^{-1}$ , where  $B^{-1}$  is a dimensionless parameter [24].

$$kB^{-1} = \ln \left( \frac{z_{0m}}{z_{0h}} \right) \quad (24)$$

Adding equations (22) and (23), equation (21) becomes:

$$r_h = \frac{1}{k u_*} \left[ \left\{ \ln \left( \frac{z-d}{z_{0m}} \right) \ln \left( \frac{z-d}{z_{0h}} \right) \right\} + \ln \left( \frac{z_{0m}}{z_{0h}} \right) \right] \quad (25)$$

Therefore, equation (20) becomes:

$$H_s = \frac{\rho c_p (T_s - T_a) k u_*}{\left[ \ln \left( \frac{z-d}{z_{0m}} \right) \ln \left( \frac{z-d}{z_{0h}} \right) + \ln \left( \frac{z_{0m}}{z_{0h}} \right) \right]} \quad (26)$$

$$z_{0m} = \frac{z-d}{e^{kK}} \quad (27)$$



$$z_{0h} = 0.1z_{0m} \quad (28)$$

The air density  $\rho$  is expressed as:

$$\rho = \frac{0.34838 P_{atm}}{T + 273.16} \quad (29)$$

where  $P_{atm}$  is the atmospheric pressure.

## 2.3 Site Description

This study was conducted at the Meteorological Station located at the Teaching and Research (T & R) Farm of the Obafemi Awolowo University, Ile-Ife, Nigeria (7.55 °N; 4.56 °E). The period of measurement was between 2016 and 2019. The climate of the study area is characterized by two distinct seasons: the dry season and the wet season. The dry season extends from November to March while the wet season runs from April to October. During the dry season, the north-easterly winds known as Harmattan, transport dry and dusty continental air masses from the Sahara desert where they originate. The wet season is characterized by frequent occurrences of rainstorms due to the high moisture content of the south-westerly airmass. The average annual precipitation at the study location ranges from about 1000 mm to 1500 mm. The study area experiences a low surface wind with a mean speed of about 2.0 ms<sup>-1</sup>, typical of tropical locations [25].

## 2.4 Instrumentation

### 2.4.1 Sensible Heat Flux

An Eddy Covariance (EC) system (shown in Fig. 1) was deployed at a height of 1.8 m for the measurement of sensible heat flux. The system consists of 3D ultrasonic anemometer (CSAT3, Campbell), CO<sub>2</sub>/H<sub>2</sub>O gas analyser (LI-7500, LI-COR) and a temperature-humidity probe, (HMP60, Vaisala) for the measurements of air temperature and humidity. The CSAT3 measured wind speed along its three orthogonal dimensions at a frequency of 10 Hz. In order to ensure that the steady-state and stationarity conditions required to achieve accuracy in measurements are met, the EC system was

positioned in such a way that the placement of the fast response sensors were in the ratio 100:1 considering the fetch area.



**Fig. 1: The Eddy Covariance System deployed at the study location**

#### 2.4.2 Routinely-Measured Meteorological Parameters

The sensors used for the measurements of the routinely-measured meteorological parameters in this study are listed in Table 1.

Variables	Sensors	Measurement Range
Solar Radiation	Pyranometer (CS300)	0 - 1750 Wm <sup>-2</sup>
Net Radiation	Net Radiometer (NR LITE)	± 2000 Wm <sup>-2</sup>
Air Temperature/ Relative Humidity	Air Temperature/Humidity Probe (HMP45)	-40 to +60 °C; 0 – 100 %
Soil Temperature	Soil Temperature Sensor (STP01)	-30 to +70 °C
Surface Temperature	Surface Sensor (RTD)	-73 to +260 °C

**Table 1: Sensors used for the Measurements of Routinely-Measured Meteorological Parameters**

## 2.5 Data Acquisition and Reduction

The instrument's manufacturer supplied a suitable software (LOGGERNET) for the programming and acquisition of the raw turbulence data acquired using the eddy covariance system. The data logging was achieved by using the Campbell Scientific

Statistical Methods	Abbreviation	Expression
datalogger system (measurement and control module) model CR 1000. The signal cables from the sensors were connected directly to the wiring panel on the CR 1000 datalogger. On the wiring panel, there are 16 SE, 8 DIFF analog input ports, 2 pulse inputs and SDM channels. A connection of the logger to the computer for communication was achieved by using USB to serial module. MircroCal Origin was used for the analysis, calculations and graphical presentation of the estimated and measured sensible heat flux. Spurious flux data were eliminated and the datasets were subjected to Quality Control (QC) and Quality Assurance (QA) protocol. The values of the measured flux were averaged to produce 30 minutes statistics.		

All the routinely-measured sensors were connected directly to a datalogger model CR10X through the SE or DIFF channels. Sampling of the data was done every 10 seconds, saved as 1-minute averaged values and subsequently, the data were reduced to produce 30 minutes statistics.

## 2.6 Statistical Methods for the Evaluation of Selected Schemes of Estimating Sensible Heat Flux

Mean Bias Error	MBE	$\frac{1}{N} \sum_{i=1}^N (E_i - M_i)$
Mean Percentage Difference	MPD	$\frac{\sum(\bar{E} - \bar{M})}{\bar{M}} \times 100 \%$
Root Mean Square Error	RMSE	$\sqrt{\frac{1}{n} \sum_{i=1}^n (E_i - M_i)^2}$
Index of Agreement	IA	$1 - \left[ \frac{\sum_{i=1}^N (E_i - M_i)^2}{\sum_{i=1}^N ( E_i - \bar{M}  +  M_i - \bar{M} )^2} \right]$
Correlation Coefficient	R	$\sqrt{\frac{\sum_{i=1}^N (E_i - \bar{E})^2 \sum_{i=1}^N (M_i - \bar{M})^2}{\sum_{i=1}^N (E_i - \bar{E})^2 \sum_{i=1}^N (M_i - \bar{M})^2}}$
Coefficient of Determination	R <sup>2</sup>	$1 - \frac{\sum_{i=1}^N (E_i - M_i)^2}{\sum_{i=1}^N (E_i - \bar{M})^2}$

**Table 2: Statistical Methods used for the Evaluation of the Performances of the Selected Schemes**

The statistical methods used for the evaluation of the performances of the schemes are listed in Table 2. The Mean Bias Error (MBE) provides the information on the tendency of a scheme to over or under predict the measured values. Positive MBE implies overestimation while negative MBE indicates underestimation of the scheme. The Mean Percentage Difference (MPD) gives the percentage of the deviances from the measured values while the Root Mean Square Error (RMSE) indicates the degree of scatter that a scheme produces. The Index of Agreement (IA) indicates the degree of conformity between the predicted and measured values. The values of IA vary between 0 and 1.

Values of IA close to 1 suggest better conformity than values close to 0. The correlation coefficient (R) and the coefficient of determination (R<sup>2</sup>) show the level of association and agreement between the estimated and measured values. Values of R and R<sup>2</sup> close to 1 indicate good fit of the scheme while values close to 0 imply a poor fit. Typically, low values of MBE, MPD, RMSE and values of R, R<sup>2</sup> and IA close to 1 are desirable for a scheme to accurately estimate the sensible heat flux.

### 3. RESULTS AND DISCUSSIONS

#### 3.1 Monthly Averages of Routinely-Measured Meteorological Parameters

The monthly average values of the routinely-measured meteorological parameters used in this study are presented in Table 3. The monthly maximum average values of solar radiation ( $217 \text{ Wm}^{-2}$ ), net radiation ( $131 \text{ Wm}^{-2}$ ) were recorded in March. March is usually a transition month between the dry and wet season. This period is characterised with occasional rain showers which leads to washouts and significant reduction in atmospheric turbidity. Consequently, there is less attenuation of the incoming radiative fluxes hence, the high values obtained. The monthly maximum average values of air temperature ( $29^{\circ}\text{C}$ ), surface temperature ( $33^{\circ}\text{C}$ ) and soil temperature ( $31^{\circ}\text{C}$ ) were recorded in February. The obtained values signify that February had the hottest weather in the study location. The maximum average value of relative humidity (88 %) was obtained in July and August. This value is attributed to the frequent occurrence of precipitation that is prominent during this period, consequently leading to high atmospheric moisture content. The maximum average value of wind speed ( $1.4 \text{ ms}^{-1}$ ) was obtained in April. This value is attributed to the occurrence of strong wind that is usually accompanied by rainfall.

The monthly minimum average values obtained for solar radiation ( $125 \text{ Wm}^{-2}$ ), net radiation ( $83 \text{ Wm}^{-2}$ ), air temperature ( $25^{\circ}\text{C}$ ), surface temperature ( $28^{\circ}\text{C}$ ) and soil temperature ( $26^{\circ}\text{C}$ ) were recorded in August. This result can be explained by the fact that August represents the 'short dry period' in the wet season and lasts for about three weeks [26]. This month experiences the cloudiest weather throughout the year, resulting in low irradiance and consequently, low air, surface and soil temperatures. The monthly minimum average value of relative humidity (64 %) was recorded in January. This value

is attributed to the dry atmospheric condition that is prevalent at this period. The monthly minimum average value of wind speed ( $0.9 \text{ ms}^{-1}$ ) at the study location was obtained in the dry season (January, October, November and December). This value shows that the dry season is a period of calm atmospheric condition.

	<b>Solar Radiation (<math>\text{Wm}^{-2}</math>)</b>	<b>Net Radiation (<math>\text{Wm}^{-2}</math>)</b>	<b>Air Temperature (<math>^{\circ}\text{C}</math>)</b>	<b>Surface Temperature (<math>^{\circ}\text{C}</math>)</b>	<b>Soil Temperature (<math>^{\circ}\text{C}</math>)</b>	<b>Relative Humidity (%)</b>	<b>Wind Speed (<math>\text{ms}^{-1}</math>)</b>
January	179	78	26	30	29	64	0.9
February	185	91	29	33	31	69	1.2
March	217	131	28	32	30	77	1.3
April	207	130	28	31	29	81	1.4
May	201	130	28	30	29	83	1.3
June	180	119	26	29	29	86	1.3
July	147	97	26	28	27	88	1.3
August	125	83	25	28	26	88	1.3
September	161	106	27	28	27	87	1.1
October	188	121	26	29	28	86	0.9
November	195	115	27	31	29	80	0.9
December	185	87	26	31	29	70	0.9

**Table 3: Monthly Averages of Routinely-Measured Meteorological Parameters**

### **3.2 Estimation of Sensible Heat Flux**

The results obtained from the different schemes both in the dry and wet seasons when compared with the measured values of  $H_s$  from the eddy covariance system is presented in Figs. 2 and 3 respectively.

In the dry season, the coefficient of determination,  $R^2$  of BP, BREB, HU and SMT are close to unity (0.9, 0.9, 0.8 and 0.9 respectively). These obtained values of  $R^2$  indicate that the estimated values obtained from the schemes show close agreements with the measured values. Thus, implying that the schemes are good fits for estimating  $H_s$  at the study location. However, the low value of  $R^2$  (0.5) obtained for ST indicates non-association of the scheme between the estimated and measured values of  $H_s$ . In the wet season, the values of  $R^2$  (0.6, 0.7, 0.6, 0.6 and 0.7) obtained from the schemes (BP, BREB, HU, SMT and ST respectively) imply a small degree of association between the predicted and measured values of  $H_s$ .

The statistics obtained from the evaluation of the schemes are presented in Table 4. From the Table, the MBE values indicate that BP, BREB, HU and SMT overestimated  $H_s$  while ST underestimated  $H_s$  both in the dry and wet seasons. The MRDs show the percentage of overestimation and underestimation by the schemes. It was observed that the over and under predictions by the schemes, were significant during the daytime (as shown in Fig. 4 for a representative day). This can be explained by the intense convective activities that are prominent during this period which causes high atmospheric instability. Similar results of BP, HU and SMT over predicting the measured values of sensible heat flux have been reported in temperate regions [27].

The overestimation of  $H_s$  using BREB has been linked to the energy partitioning investigations which revealed that BREB assumes energy terms at the surface to be balanced. Therefore, the residual term is not accounted for, by the method. As a result, the estimated values of  $H_s$  using BREB are usually higher than the measured values from the Eddy Covariance system.<sup>16</sup>

The under-estimation by the ST scheme can be linked to the surface temperature which is an important parameter in the formulation of this scheme. The values of surface

temperature are lower on a grass-covered surface due to the presence of canopy, hence minimal radiative heating. Consequently, there is a decrease in the values of  $H_s$  estimated from the ST scheme. Similar results were obtained by Stewart [28] and Adeyemi *et al.* [29]

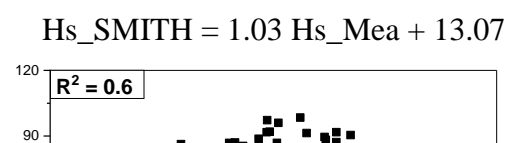
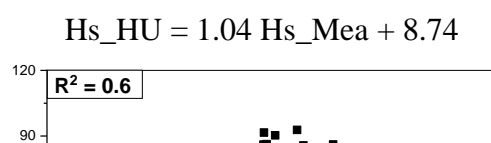
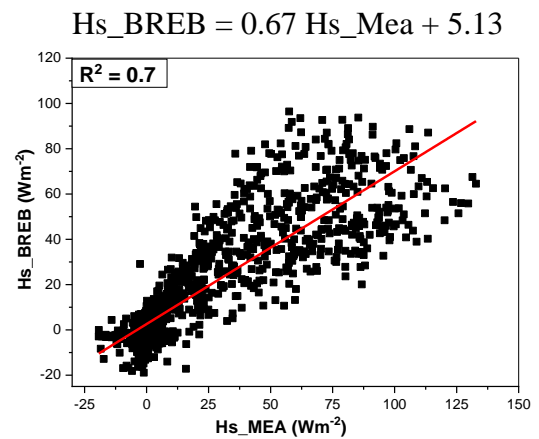
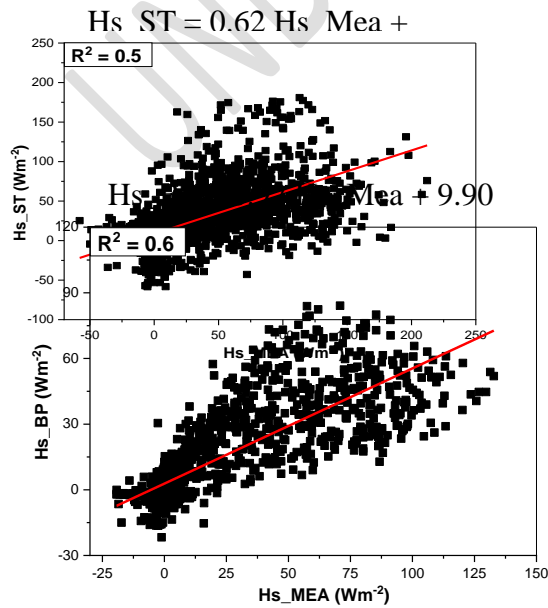
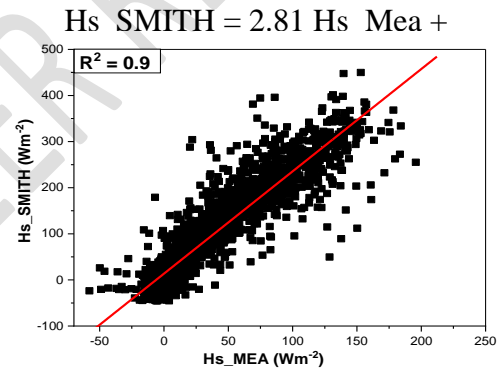
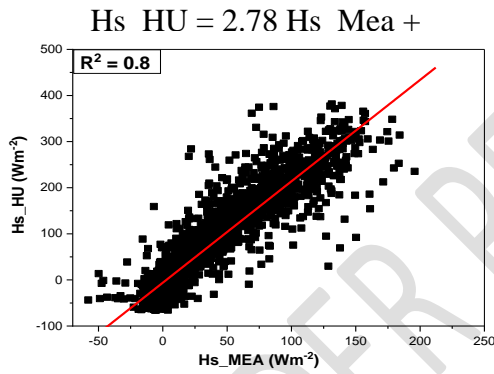
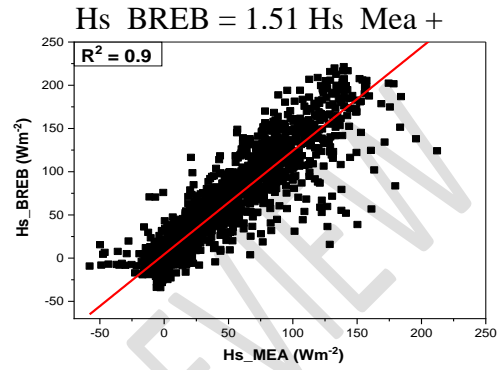
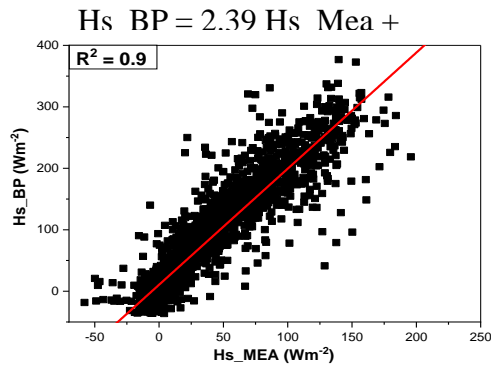




**Fig. 3: Comparison of Estimated and Measured Values of Sensible Heat Flux during the Wet Season**

Schemes	Dry Season					Wet Season				
	MBE ( $\text{Wm}^{-2}$ )	MPD (%)	R	RMSE ( $\text{Wm}^{-2}$ )	IA	MBE ( $\text{Wm}^{-2}$ )	MPD (%)	R	RMSE ( $\text{Wm}^{-2}$ )	IA

**Table 4: Statistical Evaluation of Selected Schemes of Estimating Sensible Heat Flux during the Dry and Wet Seasons**

<b>Berkowicz</b>	<b>and</b>										
<b>Prahm (BP)</b>		6.9	4.4	0.8	41.9	0.9	37.4	9.1	0.9	64.7	0.7
<b>Bowen</b>	<b>Ratio</b>										
<b>Energy</b>	<b>Balance</b>	7.2	1.7	0.9	28.7	0.9	14.2	4.1	0.9	32.3	0.9
<b>(BREB)</b>											
<b>Holstlag</b>	<b>and</b>	<b>Van</b>									
<b>Ulden (HU)</b>		7.5	7.1	0.8	52.0	0.9	4.2	28.3	0.9	72.3	0.7
<b>Smith (SMT)</b>		6.3	14.4	0.8	52.7	0.9	12.0	48.6	0.9	83.2	0.6
<b>Surface</b>											
<b>Temperature (ST)</b>		-3.8	10.7	0.8	27.3	0.9	-1.1	1.3	0.6	36.8	0.8

The RMSE values produced by the schemes during the wet season are higher (about 70 %) than those obtained during the dry season. This implies that the schemes produce high level of scatter points in the wet season than in the dry season. This is an indication that the wet season is influenced by cloudiness and high atmospheric moisture content that randomize the measurements of some crucial atmospheric variables such as the solar radiation. This in turn affects the values of sensible heat flux obtained during this period. However, the dry season is a period of clear weather conditions, hence spontaneous obtainability of atmospheric variables observed at the surface.

The IA obtained for all the schemes in both seasons are relatively good. All the schemes have the same IA value of 0.9 in the dry season signifying a good agreement of the predicted and measured values of  $H_s$  by the schemes. From the statistical evaluation, BREB has a high  $R^2$ , high R, high IA, lowest MPD, lowest RMSE and lowest MBE in both seasons, therefore, it was adjudged the best performing scheme in the study location.

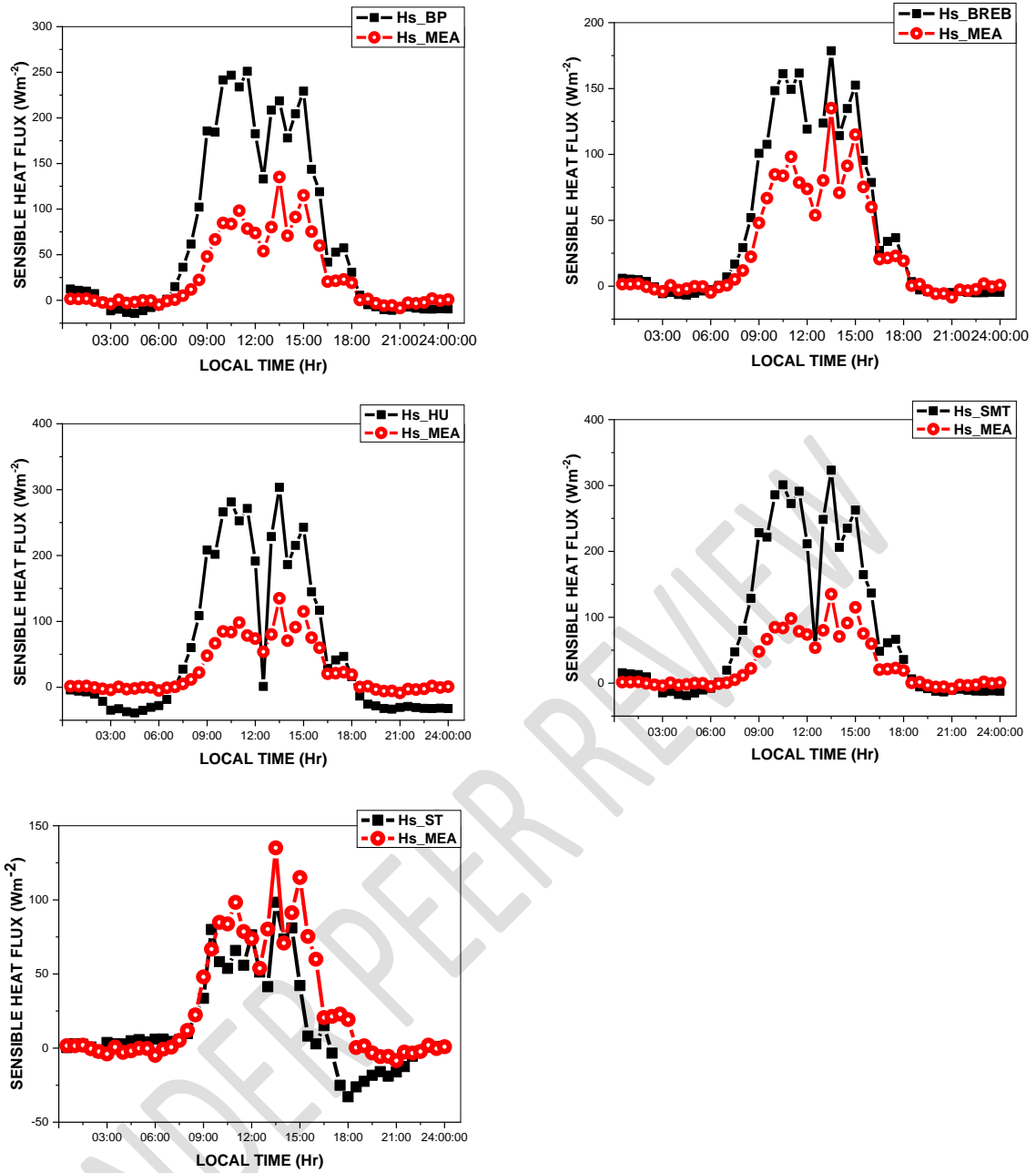


Fig. 4: Diurnal Pattern of  $H_s$  indicating the Deviances between the Estimated and Measured Values of  $H_s$

### 3.3 Validation of the Selected Schemes

The regression coefficients obtained from the least square fits of the different schemes were evaluated on a new data set (2019) for the two seasons in order to validate the

schemes. This was with the aim of improving the accuracy of the schemes. The results obtained after the validation showed significant improvements in the performances of the schemes as shown in Figs. 5 and 6 (for one representative day each) for the dry and wet seasons respectively. In the dry season, MBE values of  $7.0 \text{ Wm}^{-2}$ ,  $12.4 \text{ Wm}^{-2}$ ,  $7.0 \text{ Wm}^{-2}$ ,  $15.4 \text{ Wm}^{-2}$  and  $-2.7 \text{ Wm}^{-2}$  were calculated for BP, BREB, HU, SMT and ST respectively before validation and then reduced to  $1.9 \text{ Wm}^{-2}$ ,  $2.3 \text{ Wm}^{-2}$ ,  $2.4 \text{ Wm}^{-2}$ ,  $1.0 \text{ Wm}^{-2}$  and  $1.6 \text{ Wm}^{-2}$  respectively after validation.

Also, in the wet season, the MBEs obtained for BP, BREB, HU, SMT and ST before validation are  $22.7 \text{ Wm}^{-2}$ ,  $19.2 \text{ Wm}^{-2}$ ,  $34.6 \text{ Wm}^{-2}$ ,  $30.5 \text{ Wm}^{-2}$  and  $-22.4 \text{ Wm}^{-2}$  respectively. After adjustment, the MBEs reduced to  $9.6 \text{ Wm}^{-2}$ ,  $4.4 \text{ Wm}^{-2}$ ,  $8.7 \text{ Wm}^{-2}$ ,  $6.3 \text{ Wm}^{-2}$  and  $-2.3 \text{ Wm}^{-2}$  for BP, BREB, HU, SMT and ST respectively.

The improvements obtained from the validation imply that the schemes will produce accurate estimations of sensible heat flux when the obtained regression coefficients are employed in the schemes. This in turn will improve the applicability of sensible heat flux in the surface energy budget at a tropical location.

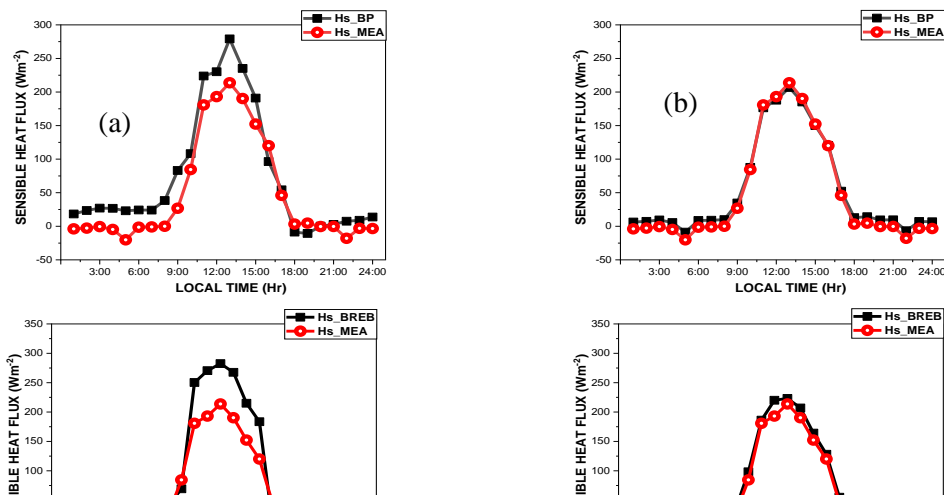
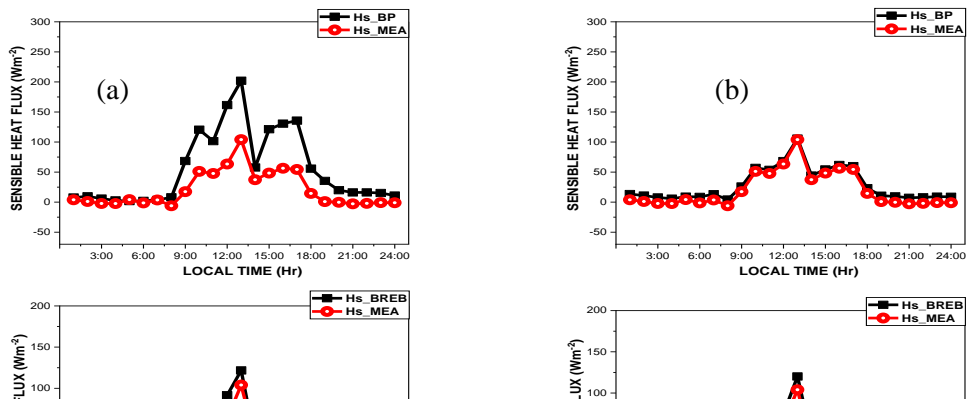




Fig. 5: Selected Schemes of Estimating  $H_s$  (a) Before and (b) After Validation in the Dry Season





**Fig. 6: Selected Schemes of Estimating  $H_s$  (a) Before and (b) After Validation in the Wet Season**

#### **4. SUMMARY AND CONCLUSION**

In this study, the performances of selected empirical schemes for calculating sensible heat flux based on routinely-measured meteorological parameters at a tropical site inside the Teaching and Research farm (7.55 °N; 4.56 °E) of Obafemi Awolowo University, Ile-Ife, Nigeria; have been evaluated. The direct measurement of sensible heat flux was obtained from an Eddy Covariance (EC) system set up at the same study location and used as benchmark for validation of the different schemes.

The schemes that were selected for calculating sensible heat flux in this study are the aerodynamic resistance schemes such as: Berkowicz and Prahm (BP), Holstlag and Van Ulden (HU), Smith and Surface Temperature (ST) schemes; and the Bowen Ratio Energy Balance (BREB). The choice of selecting these schemes was due to the availability of data for the various input parameters. The period of estimation was from 2016 to 2018.

The result from the estimation of the schemes revealed that the MBE values of  $6.9 \text{ Wm}^{-2}$ ,  $7.2 \text{ Wm}^{-2}$ ,  $7.5 \text{ Wm}^{-2}$ ,  $6.3 \text{ Wm}^{-2}$  and  $-3.8 \text{ Wm}^{-2}$  were obtained for BP, BREB, HU, SMT and ST respectively in the dry season. In the wet season, BP, BREB, HU, SMT and ST had MBE values of  $37.4 \text{ Wm}^{-2}$ ,  $14.2 \text{ Wm}^{-2}$ ,  $4.2 \text{ Wm}^{-2}$ ,  $12.0 \text{ Wm}^{-2}$  and  $-1.1 \text{ Wm}^{-2}$  respectively. The MBE and RMSE values were higher in the wet season than in the dry season. This implies that the schemes performed better in the dry season than in the wet season. Also, the over and under prediction of the schemes were prominent during the day time due to the atmosphere being unstable at this period. The study rated BREB as the best performing scheme in the study location. In order to improve the accuracy of the schemes, the regression coefficients obtained from the least square fits of the schemes, were applied on a new data set in year 2019 in order to validate the schemes. The result showed significant improvements in the schemes which is of great importance in the application of sensible heat flux.

## REFERENCES

1. Gentine P, Entekhabi D and Heusinkveld B. Systematic errors in ground heat flux estimation and their correction. *Water Resour. Res.* 2012;48:W09541, doi:10.1029/2010WR010203
2. Xu T, Bateni SM, Liang S, Entekhabi D and Mao K. Estimation of surface turbulent heat fluxes via variational assimilation of sequences of land surface temperatures from Geostationary Operational Environmental Satellites. *J. Geophys. Res. Atmos.* 2014;119:780–798.
3. Schmid HP, Cleugh HA, Grimmond CS and Oke TR. Spatial variability of energy fluxes in suburban terrain. *Bound. Layer Meteorol.* 1991;54:249–276.
4. Beringer J and Tapper N. Surface energy exchanges and interactions with thunderstorms during the Maritime Continent Thunderstorm Experiment (MCTEX). *J. Geophys. Res.* 2002;107:4552–4564.
5. Arya SP. *Introduction to Micrometeorology*. Academic Press, San Diego, 2001.
6. Yuan G, Zhang L, Liang J, Cao X and Zhaohong Y. Understanding the partitioning of the available energy over the semi-arid areas of the Loess Plateau, China, *Atmosphere*. 2017;87; doi:10.3390/atmos8050087.
7. Katavoutas G, Flocas H and Tsitsomitsiou. Thermal comfort in hot outdoor environment under unsteady conditions. *Advances in Meteorology, Climate and Atmospheric Physics, Greece*. 2014; 2:195-200.
8. Li X, Gao Z, Li Y and Tong B. Comparison of Sensible Heat Fluxes Measured by a Large Aperture Scintillometer and Eddy Covariance System over a Heterogeneous Farmland in East China. *Atmosphere*. 2017;8:101; doi:10.3390/atmos8060101.
9. Aubinet M, Grelle A, Ibrom A, Rannik U, Moncrieff J, Foken T et al. Estimates of the annual net carbon and water exchange of forests: the EUROFLUX methodology. *Advanced Ecology Research*. 2002;30:113–175.
10. Jerald AB and Kenneth CC. Examination of the surface energy budget: A comparison of eddy-correlation and Bowen ratio measurement system, *J. Hydro meteorol.* 2020;4:160.
11. Massman WJ and Lee X. Eddy covariance flux corrections and uncertainties in long-term studies of carbon and energy exchanges. *Agriculture Forestry Meteorological Society*. 2002;134:1-10.
12. Hoedjes J, Chehbouni A, Ezzachar J, Escadafal R and De Bruin H. Comparison of large aperture scintillometer and eddy covariance measurements: Can thermal infrared data be used to capture footprint-induced differences? *J. Hydrometeorol* 2007;8:144 – 159.



13. Berkowicz R and Prahm LE. Sensible heat flux estimated from routine meteorological data by the resistance method. *J. Appl. Meteorol.* 1982;21:1845-1864.
14. Foken T and Wichura B. Tools for quality assessment of surface-based flux measurements. *Agric. For. Meteorol.* 1996;78: 83 - 105.
15. Balogun AA, Jegede OO, Foken T and Olaleye JO. Estimation of sensible and latent heat fluxes over bare soil using Bowen ratio energy balance method at a humid tropical site. *Journal of the African Meteorological Society.* 2002; 5(1): 63-71.
16. Kakane V and Agyei E. Determination of surface fluxes using a Bowen ratio system. *West Africa Journal of Applied Ecology.* 2006; 0855-4307.
17. Jegede OO, Foken T, Balogun EE and Abimbola OJ. Bowen ratio determination of sensible and latent heat fluxes in a humid tropical environment at Ile-Ife, Nigeria. *Mausam.* 2001; 52(4):669-678.
18. Foken T. The energy balance closure problem – An overview. *Ecolog. Appl.* 2008; 18.
19. Bernhofer C. Estimating forest evapotranspiration at a non-ideal site. *Agric Forest Meteorol.* 1992;60:17–32.
20. Barr AG, King KM, Gillespie TJ, Denhartog G and Neumann HN. A comparison of Bowen ratio and eddy correlation of sensible and latent heat flux measurements above deciduous forest. *Boundary Layer Meteor.* 1994; 71:21–41.
21. Holtslag AA and Van Ulden AP. A simple scheme for daytime estimates of the surface fluxes from routine weather data. *J. Clim. Appl Meteorol.* 1983;22:517-529.
22. Smith FB. Atmospheric Structure. Unpublished note presented at Air Pollution Modeling for Environmental Impact Assessment, International Centre for Theoretical Physics, Trieste. 1990.
23. Hall FG, Huemmrich KF, Goetz SJ, Sellers PJ and Nickeson JE. Satellite remote sensing of surface energy balance: Successes, failures and unresolved issues in FIFE. *J. Geophys. Res.* 1992;97:61 - 89.
24. Cordova M, Bogerd L, Smeets P and Carrillo-Rojas G. Estimating turbulent fluxes in the tropical Andes. *Atmosphere.* 2020;11:213, doi:10.3390/atmos11020213.
25. Ayoola MA, Sunmonu LA, Bashiru MI and Jegede, OO. Measurements of net all-wave radiation at a tropical location, Ile-Ife, Nigeria. *Atmosfera.* 2014;27 (3): 305 – 315.

26. Obisesan OE. Estimation of Atmospheric Turbidity Parameters in Ile-Ife, Nigeria, *Physical Science International Journal*. 2021;25(7):30-40; doi: 10.9734/PSIJ/2021/v25i730270.
27. Andreas EL, Horst TW, Grachev AA, Persson PO, Fairall CW, Guest PS and Jordan RE. Parametrizing turbulent exchange over summer sea ice and the marginal ice zone. *Q. J. R. Meteorol. Soc.* 2010;136:927 - 943, doi: 10.1002/qj.618.
28. Stewart JB. Turbulent surface fluxes derived from radiometric surface temperature of sparse prairie grass. *J. Geophys. Res.*1995;100:429 – 433.
29. Adeyemi B, Ogolo EO and Ajakaiye MP. Parameterization of convective heat fluxes over Ile-Ife using Bowen ratio, aerodynamic gradient and aerodynamic with resistance techniques. *International Journal of Applied Science - Research and Review*. 2017;4:2-11, doi: 10.21767/2394-9988.100061.